Production of neutron-rich Λ hypernuclei by double-charge-exchange reactions

T.Yu. Tretyakova[a] and D.E. Lanskoy[b]

[a] *Frank Laboratory of Neutron Physics, JINR, 141980 Dubna, Moscow region, Russia*

[b] *Institute of Nuclear Physics, Moscow State University, 119992 Moscow, Russia*

Abstract

We calculate cross sections of production of neutron-rich hypernuclei by the ${}^{A}\mathrm{Z}(\pi^-, K^+)^{A}_{\Lambda}(\mathrm{Z}{-}2)$ and ${}^{A}\mathrm{Z}(K^-, \pi^+)^{A}_{\Lambda}(\mathrm{Z}{-}2)$ reactions. Structure studies of neutron-rich hypernuclei attainable in these reactions have shown that their properties are sensitive to delicate features of hypernuclear interactions. We consider two mechanisms of the reactions. The first mechanism is a two-step process with meson charge exchange (e.g., $\pi^- p \to \pi^0 n$, $\pi^0 p \to K^+\Lambda$). Another mechanism is one-step production ($\pi^- p \to K^+\Sigma^-$) proceeding via a small Σ^- component, arising in Λ hypernuclei due to $\Lambda n - \Sigma^- p$ coupling, as a doorway state. Typically, the two-step mechanism is more productive. We predict the differential cross sections for various light targets. A relatively large cross section at zero angle is found for the ${}^{10}\mathrm{B}(\pi^-, K^+)^{10}_{\Lambda}\mathrm{Li}$ reaction.

1 Introduction

Hypernuclei with neutron excess relate both to physics of exotic nuclei and to strangeness nuclear physics. On the one hand, neutron-rich hypernuclei give information about response of loosely bound nuclear systems to Λ induced perturbation. Some unbound neutron-rich nuclei can be bound by Λ hyperon. So studying of such systems can enrich our knowledge on exotic, especially neutron-halo, nuclei.

On the other hand, extension of hypernuclear chart is of considerable importance for physics of hyperonic interactions. Properties of neutron-rich Λ hypernuclei appear to be sensitive to subtle features of ΛN interaction in nuclear medium hardly deduced from "usual" hypernuclei. We have studied theoretically [1] several examples of neutron-rich Λ hypernuclei (like $^{12}_{\Lambda}\mathrm{Be}$, $^{16}_{\Lambda}\mathrm{C}$, $^{11}_{\Lambda}\mathrm{Li}$) and have shown that the separation energies of the last neutron are affected by a delicate interplay between ΛN density-dependent force, polarization of the nuclear core by the hyperon, and the spin-orbit neutron-nucleus potential.

The $^{12}_{\Lambda}\mathrm{Be}$ hypernucleus is an impressive example of influence of ΛN interaction features on neutron halo response to hyperon addition. We use the Skyrme-Hartree-Fock approach allowing us to take into account the action of hyperon not only on the halo neutron, but also on inner nucleons named the core.

The ground ($1/2^+$) and the first excited ($1/2^-$) bound states of ${}^{11}\mathrm{Be}$ are treated as pure neutron $2s_{1/2}$ and $1p_{1/2}$ states, correspondingly, near the core ${}^{10}\mathrm{Be}(0^+)$. For simplicity the possible configuration mixing is ignored. The neutron single particle energies e_n as well as rms radii of the nuclear core and the last neutron orbit are presented in fig. 1 for various ΛN interactions. We present the results for three parameter sets, which produce different polarization of the core ${}^{10}\mathrm{Be}$. The 5th set from [2] (YBZ5) furnishes a good agreement with experimental Λ binding energies, it involves the ΛNN force of moderate strength and, therefore, leads to a slight polarization. The SKSH1 set [3] includes no ΛNN force, so the interaction is core-contracting. The third one is the 3rd parameter set from [4] (hereafter R3) with a huge ΛNN force, which exemplifies a core-diluting interaction.

It is seen that the $1p_{1/2}$ halo state energy in $^{12}_{\Lambda}\mathrm{Be}$ is quite sensitive to the ΛN interaction. Contrary to the behaviour of usual compact nuclei, the hyperon addition pushes the halo state upward to the threshold in the case of core-contracting interaction SKSH1. Otherwise, the core-diluting R3 set gives a well-bound $1p_{1/2}$ state which becomes the ground state of $^{12}_{\Lambda}\mathrm{Be}$. The nonpolarizing YBZ5 set represents an intermediate case. Evidently, the neutron separation energy is strongly correlated with the polarizing property of the ΛN interaction. For details of interplay between features of potentials acting on halo neutron and structure of hypernuclei with neutron excess see [1].

Above, we discussed polarization of the compact core ${}^{10}\mathrm{Be}$, which is related to properties of the ΛN interaction in the usual way. As for the whole host nucleus ${}^{11}\mathrm{Be}$, its polarization is of different type, inherent for loosely bound nuclei. Since the core and halo radii change oppositely (see the values in fig.1), the total radius of ${}^{11}\mathrm{Be}$ remains almost unchanged for the SKSH1 interaction and is reduced for the R3 forces. In contrast to usual compact hypernuclei for such systems the strongest contraction corresponds to ΛN interaction with three-body forces and it may achieve 9% for $^{12}_{\Lambda}\mathrm{Be}$. Similar result was obtained earlier

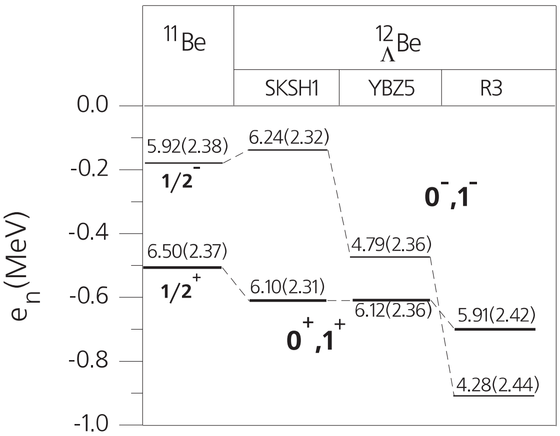

Figure 1: External neutron single-particle energies e_n (MeV) and corresponding rms radii (fm) of the last neutron in $^{12}_{\Lambda}$Be and the core ^{10}Be (in parentheses). ΛN interactions are SKSH1, YBZ5 and R3. NN interaction is Sk3. Thick lines are for $2s$ halo states, and thin ones are for $1p$ state.

for cluster systems [5] and glue-like role of the Λ hyperon for light loosely bound nuclei was pointed out in [6]. The single experimental result for polarization (contraction) of host nucleus by hyperon corresponds to cluster system $^{7}_{\Lambda}$Li and it is about 19% [7].

Usually, Λ hypernuclei are formed in the (K^-,π^-) and (π^+,K^+) reactions, where elementary processes like $K^-n\to\pi^-\Lambda$ occur on a neutron inside a nucleus. The target charge remains unchanged in this case. For production of neutron-rich hypernuclei, reactions (K^-,π^+) and (π^-,K^+) are suitable [8], but the underlying mechanisms are more complicated. We consider two possible mechanisms: the two-step process with charge exchange, for example, $K^-p\to\pi^0\Lambda$, $\pi^0p\to\pi^+n$, and the second one, production of Λ hypernuclei in the one-step process like $K^-p\to\pi^+\Sigma^-$ via small admixture of the virtual Σ^- state appearing due to $\Sigma^-p\leftrightarrow\Lambda n$ coupling. Similarly to the "usual" reactions, the (K^-,π^+) one can be executed by stopped kaons (via kaonic capture from an atomic orbit) as well as in flight, using kaonic beams with momenta about 1 GeV/c or lower. Pion-induced production is possible only in flight and requires an incident momentum not less than ~ 0.9 GeV/c.

Below we consider all three reactions, in which typical neutron-rich Λ hypernuclei like $^{16}_{\Lambda}$C, $^{12}_{\Lambda}$Be, $^{11}_{\Lambda}$Li, $^{10}_{\Lambda}$Li and $^{9}_{\Lambda}$He can be produced. We consider production of $^{12}_{\Lambda}$Be and $^{16}_{\Lambda}$C from ^{12}C and ^{16}O targets respectively and focus mainly on the former, as the production rates of $^{12}_{\Lambda}$Be appear to be higher. We address also the ^{10}B$(\pi^-,K^+)^{10}_{\Lambda}$Li reaction, which is induced by the recent KEK experiment [9]. The paper is organized as follows. In the next section we present our calculations for Σ^- admixture in $^{12}_{\Lambda}$Be and rates of its production by stopped kaons as well as kaon- and pion-induced reactions in flight. Two-step mechanism of the (π^-,K^+) production of $^{12}_{\Lambda}$Be, $^{16}_{\Lambda}$C and $^{10}_{\Lambda}$Li is analyzed in Sec. 3. The last section is devoted to some conclusion.

2 One-step production via Σ^- admixture

The significant role of $\Lambda\Sigma$ coupling in light hypernuclei was shown in [10]. This coupling becomes more effective in systems with neutron excess and affects interactions in high-density nuclear matter, like neutron stars [11].

We treat a hypernuclear state as a superposition of the main Λ component and a small Σ admixture, which serves as a doorway state. For example,

$$\left|^{12}_{\Lambda}\mathrm{Be}\right\rangle=\psi_\Lambda+\psi_\Sigma, \tag{1}$$

where $\psi_\Lambda=\alpha\left|^{11}\mathrm{Be}\otimes\Lambda\right\rangle$ and $\psi_\Sigma=\beta\left|^{11}\mathrm{B}\otimes\Sigma^-\right\rangle$. The one-step production considered is direct formation of the second component of (1).

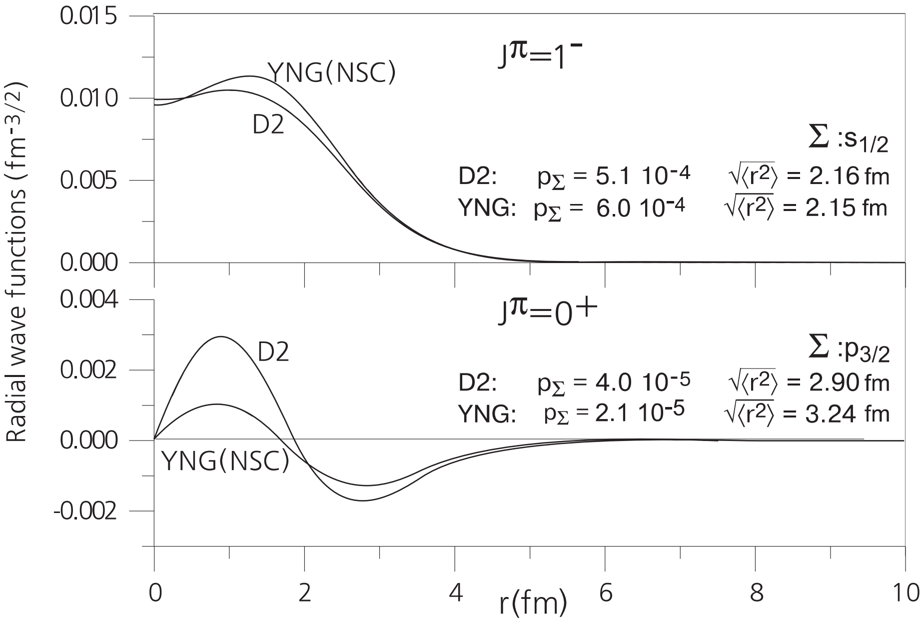

Figure 2: Radial wave functions u_Σ/r of Σ admixture in ${}^{12}_{\Lambda}$Be.

In principle, we have a two-channel problem:

$$\left\{ \begin{array}{rcrcl} (T_\Lambda + U_{\Lambda\Lambda})\psi_\Lambda & + & U_{\Sigma\Lambda}\psi_\Sigma & = & e_\Lambda\psi_\Lambda \\ U_{\Sigma\Lambda}\psi_\Lambda & + & (T_\Sigma + U_{\Sigma\Sigma})\psi_\Sigma & = & e_\Sigma\psi_\Sigma, \end{array} \right. \tag{2}$$

where notations are self-explanatory. We solve the second equation alone (perturbatively), using the energy and the Λ wave function calculated in the single-channel Hartree-Fock approach [1] with phenomenological ΛN potential (set 1 from [2]) fitting well Λ hypernuclear spectra [12]. Our goal is not to study influence of the Σ admixture on Λ hypernuclear states but rather to find the admixture in the specific channel effective for the production. Then, treating the system in each channel as the inert core and two independent particles, we come to the following equation for Σ radial wave function $u_\Sigma(r)$:

$$\left(-\frac{1}{2\mu_\Sigma}\frac{d^2}{dr^2} + \frac{l(l+1)}{2\mu_\Sigma r^2} + U_{\Sigma\Sigma}(r) - e_\Sigma \right) u_\Sigma(r) = S(r). \tag{3}$$

Here source term $S(r)$ arises from two-particle coupling interaction $\Sigma^- p \leftrightarrow \Lambda n$. Calculation of $S(r)$ was performed using the Hartree-Fock single-particle wave functions.

The salient feature of this equation is a rather large magnitude of energy e_Σ (about -80 MeV), which involves the mass difference between Σ and Λ. As we shall see later, it implies some distinctive properties of the solutions. Note here that with such e_Σ, the wave function $u_\Sigma(r)$ falls as $S(r)$ at large r, but not as $\exp(-\sqrt{2\mu_\Sigma|e_\Sigma|}r)$ as usual.

We employ two central coupling potentials: first we use potential D2 from [10], which simulates the ND potential [13] and gives the same phases of hyperon-nucleon scattering at low energies. This potential succeeds in simultaneous description of binding energies of s shell hypernuclei [10]. The second potential is the G-matrix YNG interaction by Yamamoto (cited in [14]), obtained from the NSC-89 model [15]. For the diagonal Σ-nucleus potential $U_{\Sigma\Sigma}(r)$ we adopt the real part of a density dependent potential from [16] fitted to Σ^- atomic data.

The Σ radial wave function $u_\Sigma(r)/r$ in the $J = 1^-$ state of ${}^{12}_{\Lambda}$Be is shown in the upper part of fig. 2. In this case, the halo neutron moves in the $1p_{1/2}$ state and the hyperon is in the $1s_{1/2}$ state. For both the coupling potentials, the Σ admixture probability is as small as about 0.05%. It is considerably smaller than p_Σ's from several tenths to 2% obtained in various approaches for s shell Λ hypernuclei [10, 17]. Probably the main reason of this difference is the halo-like behavior of the coupled neutron in our case, which implies a small overlap of neutron distribution with other baryons. Moreover, we deal with p shell hypernuclei in which the coupling involves baryons from different shells.

It is seen that Σ hyperon is displaced from the center owing to the coupling with the peripheral halo state. On the other hand, it is not an usual peripheral state. The spatial distribution falls rapidly outside of the nucleus and concentrates just at the edge of the nucleus. The rms radius is as small as 2.16 fm (less than the rms radius of ^{10}Be). Such spatial distributions are favorable for production, since there is strong meson absorption in the center.

The lower part of fig. 2 presents the Σ wave function in the 0^+ state of $^{12}_{\Lambda}$Be with $2s$ neutron halo. Here the probabilities are still smaller since Λ and neutron are in the pure singlet state in our model whereas the singlet coupling interaction is known to be weaker than the triplet one. The peculiar feature of this state is the node of the Σ wave function induced by the node of the neutron $2s$ state. So the Σ state is $2p$-like here. The rms radius is again relatively small.

To calculate rates of the hypernuclear production by stopped kaons, we adopt the standard approach suggested in Ref. [18]. The production rate is proportional to the squared matrix element:

$$R \sim \left| \left\langle \chi_\pi, \psi_\Sigma \left| \sum_{i=1}^{Z} t_i(K^- p \to \Sigma^- \pi^+) X(i) \right| \varphi_K, {}^{12}\mathrm{C} \right\rangle \right|^2 , \tag{4}$$

where χ_π is the distorted π^+ wave, φ_K is the atomic K^- wave function, $t_i(K^- p \to \Sigma^- \pi^+)$ is the amplitude of the elementary reaction, which is supposed to be zero-range and spin-independent, and $X(i)$ is the operator converting $p \to \Sigma^-$. For estimating purpose, we use the simple Coulomb wave function for the kaon. Pion distortion is taken into account in the eikonal approximation. Following Ref. [19] we rely that kaon absorption occurs from 3D (80%) and 2P (20%) atomic orbits, and the total yield of the $K^- p \to \pi^+ \Sigma^-$ reaction in the nuclei is twice as large as that of the $K^- n \to \pi^- \Lambda$ reaction. In order to minimize various uncertainties in the rate calculations, we present the ratios of the rates per a stopped kaon of the reactions $^{12}\mathrm{C}(K^-, \pi^+)^{12}_{\Lambda}\mathrm{Be}$ and $^{12}\mathrm{C}(K^-, \pi^-)^{12}_{\Lambda}\mathrm{C}$, calculated in the same approach for the states with the same quantum numbers:

$$X = \frac{R[^{12}\mathrm{C}(K^-, \pi^+)^{12}_{\Lambda}\mathrm{Be}(J^\pi, p^{-1}(l_1 j_1)\Sigma^-(l_2 j_2))]}{R[^{12}\mathrm{C}(K^-, \pi^-)^{12}_{\Lambda}\mathrm{C}(J^\pi, n^{-1}(l_1 j_1)\Lambda(l_2 j_2))]}, \tag{5}$$

as was suggested in [20]. In the Table 1, the ratios for the 2 states of $^{12}_{\Lambda}$Be are shown.

Table 1: Σ admixture probabilities p_Σ in $^{12}_{\Lambda}$Be, rate ratios X and production rates for coupling potentials YNG and D2.

	J^π	p_Σ	X	Production per kaon
YNG	1^-	$6.0 \cdot 10^{-4}$	$1.3 \cdot 10^{-3}$	$1.3 \cdot 10^{-6}$
	0^+	$2.1 \cdot 10^{-5}$	$7.3 \cdot 10^{-5}$	$9.3 \cdot 10^{-8}$
D2	1^-	$5.1 \cdot 10^{-4}$	$1.2 \cdot 10^{-3}$	$1.2 \cdot 10^{-6}$
	0^+	$4.0 \cdot 10^{-5}$	$1.2 \cdot 10^{-4}$	$1.6 \cdot 10^{-7}$

Production rates per a stopped kaon in Table 1 are estimated using calculated X and the experimental rates of the (K^-, π^-) reaction obtained at KEK [21]. Our crude estimations for production of the same states by the two-step charge exchange mechanism gave values higher by an order of magnitude ($1.8 \cdot 10^{-5}$ for 1^- state and $6.0 \cdot 10^{-6}$ for sum of 0^+ and 1^+ states; note that in contrast to the one-step mechanism, the two-step process can excite unnatural parity states too). For the experimental production rate of the $^{12}\mathrm{C}(K^-, \pi^+)$ reaction the upper limits about $6 \cdot 10^{-5}$ [22] and very recent preliminary result from DAΦNE $2.1 \cdot 10^{-5}$ [23] are known.

For differential cross sections of the (π^-, K^+) and (K^-, π^+) reactions in flight within the one-step mechanism we adopt the usual DWIA approach, which is widely applied to the similar (π^+, K^+) and (K^-, π^-) reactions (e.g., [24]). In fig. 3, the differential cross sections of the $^{12}\mathrm{C}(\pi^-, K^+)$ reaction at 1.05 GeV/c are shown. The cross sections are typically less than 1 nb/sr and are in accordance with p_Σ

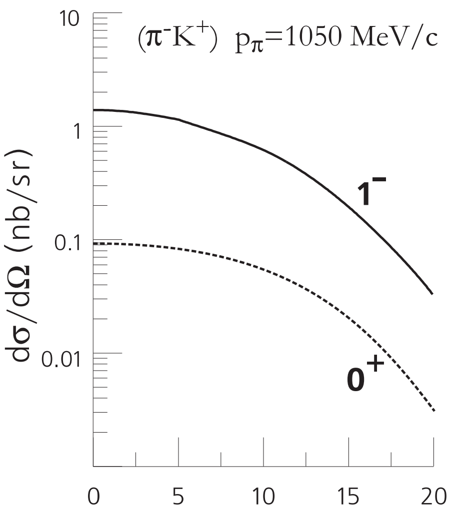

Figure 3: Differential cross sections of the ${}^{12}\mathrm{C}(\pi^-, K^+){}^{12}_{\Lambda}\mathrm{Be}$ reaction. One-step mechanism via Σ admixture.

values listed in Table 1. The (π, K) reaction is characterized by a fairly high momentum transfer (about 350 MeV/c) even at zero angle, so the angular dependence of the cross sections is rather simple.

In fig. 4, the cross sections of the ${}^{12}\mathrm{C}(K^-, \pi^+){}^{12}_{\Lambda}\mathrm{Be}$ reaction are depicted at two incident kaon momenta. The momentum 500 MeV/c corresponds to near-recoilless kinematics at zero angle (the momentum transfer is almost zero). So the $0^+ \to 0^+$ transitions dominate at $\theta = 0$ despite less p_Σ's. Nonzero-spin states can be produced at larger angles. At 900 MeV/c (zero-angle momentum transfer is about 100 MeV/c), production of the 1^- state prevails in the whole range of angles considered.

The cross sections of the (K^-, π^+) reaction reach 100 nb/sr. This does not mean that this reaction is more feasible, since available kaonic beams are much less intensive than pionic ones. However, comparison of figs. 3 and 4 shows that the kinematics of the (K^-, π^+) reaction is more selective due to wide possibilities to vary the momentum transfer.

3 Two-step mechanism of the (π^-, K^+) reaction

Treating the two-step mechanism ($\pi^- p \to \pi^0 n, \pi^0 p \to K^+ \Lambda$ and $\pi^- p \to K^0 \Lambda, K^0 p \to K^+ n$), we utilize the Glauber approach. For one-step reactions it gives essentially the same description as the DWIA at energies about 1 GeV, whereas its extension to two-step processes is straightforward.

The cross section of the $N(\pi, K)\Lambda$ elementary reaction is sharply peaked at the incident momentum $p_\pi = 1.05$ GeV/c (while the cross section of the $p(\pi^-, K^+)\Sigma^-$ reaction varies smoothly with the momentum), so the largest cross sections might be expected at this momentum value. As the momentum transfer in the (π, K) reactions is high already at zero angle and increases further with angle, we present here only the results at $\theta = 0$ (the cross sections of the two-step mechanism fall with angle). In Table 2 the cross sections calculated within the two-step mechanism [25] are presented. The results for the one-step process are also shown for comparison.

It is seen that the two-step cross sections exceed considerably (excepting ${}^{16}_{\Lambda}\mathrm{C}$ (2^+) production) the one-step ones. So it may be suggested that the two-step mechanism is more effective, at least for the hypernuclei considered.

Note that the cross sections in Table 2 are calculated for the two-step and one-step mechanisms separately. Strictly speaking, one should sum the amplitudes rather than the cross sections. However, the relative phase between the amplitudes of the mechanisms is unknown and hardly deduced. When the contributions of two mechanisms differ substantially from each other, this problem is not significant.

In connection with the experiment recently carried out at KEK [9], we calculate the cross section of the ${}^{10}\mathrm{B}(\pi^-, K^+){}^{10}_{\Lambda}\mathrm{Li}$ reaction within the two-step mechanism (it is presumed to be dominant). We

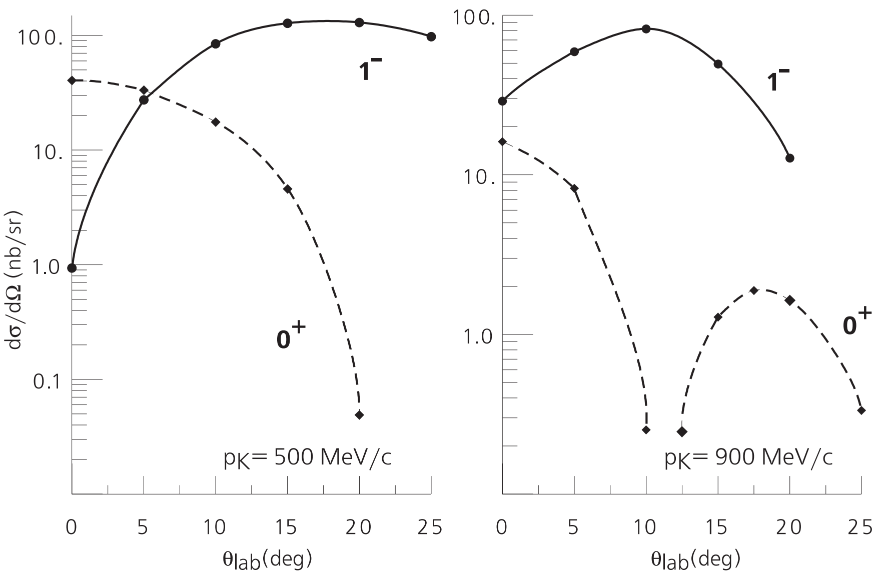

Figure 4: Differential cross sections of the $^{12}\mathrm{C}(K^-,\pi^+)^{12}_{\Lambda}\mathrm{Be}$ reaction. One-step mechanism via Σ admixture.

Table 2: Differential cross sections (nb/sr) of (π^-, K^+) reaction at zero angle at $p_\pi = 1.05$ GeV/c.

	J^π	two-step mechanism	one-step mechanism
$^{12}_{\Lambda}\mathrm{Be}$	1^-	6.5	1.4
	0^+	2.1	0.1
$^{16}_{\Lambda}\mathrm{C}$	2^+	0.4	0.3
	0^+	0.1	0.01
$^{10}_{\Lambda}\mathrm{Li}$	2^-	66.8	
	1^-	3.2	

consider two states (1^- and 2^-) built on the ground state of ^{9}Li ($3/2^-$). It is seen from Table 2 that the cross section for $^{10}_{\Lambda}$Li (2^-) production is much higher than for all the other cases.

In $^{12}_{\Lambda}$Be and $^{16}_{\Lambda}$C production, nucleon undergone the charge exchange is forced to change its state drastically. Quantum numbers of the external neutron always differ from quantum numbers of the protons. Moreover, the spatial distribution of the external (halo) neutron overlaps poorly with the distributions of the core protons. Such a drastic change is not needed for the $^{10}_{\Lambda}$Li production. Furthermore, in the two-step transition (e.g., $^{10}\mathrm{B}(3^+) \rightarrow ^{10}_{\Lambda}\mathrm{Be}(2^-) \rightarrow ^{10}_{\Lambda}\mathrm{Li}\ (2^-)$), the charge-exchange step can proceed without angular momentum transfer. That is why production of $^{10}_{\Lambda}$Li (2^-) is enhanced.

The first experiment on the $^{10}_{\Lambda}$Li production gave 5.8 ± 2.2 nb/sr and 11.3 ± 1.9 nb/sr at 1.05 GeV/c and 1.2 GeV/c incident momentum, respectively [9], and smaller cross sections for the $^{12}_{\Lambda}$Be production. The results support our predictions of enhanced $^{10}\mathrm{B}(\pi^-, K^+)^{10}_{\Lambda}\mathrm{Li}$ reaction rate, but quantitatively the agreement is relatively poor. It should be noted that indicated cross sections are not of same meanings strictly, since integration over the whole interval $0 < B_\Lambda < 15$ MeV has been performed in experiment. Also the experimental cross sections are averaged over the scattering angle from 2 to 14 degree.

The main qualitative disagreement is in the energy dependence of the cross sections. We predicted the cross section about 33.7 nb/sr at $p_\pi = 1.2$ GeV/c, which is considerably less than that at $p_\pi = 1.05$ GeV/c according to the sharp peak of the cross section of the elementary $\pi N \rightarrow K\Lambda$ reaction. The experimental ratio is nearly inverse. The energy dependence is an open problem now.

Hypernucleus $^{10}_{\Lambda}$Li is built on relatively tightly bound core ^{9}Li and does not represent extremely neutron-rich (halo) systems. But the system possesses a considerable neutron excess (N/Z = 2), and its detection is of great interest as the first step in the program of study of neutron-rich hypernuclei [9, 26].

4 Conclusion

Production of neutron-rich Λ hypernuclei, was being a rather speculative topic a decade ago, now enters a practical stage. After the first attempt [22], which gave only upper limits for production rates, the first successful experiment [9] has been performed at KEK with pionic beam. Our calculations [25] were induced to a considerable extent by the experimental challenge and helped to propose the feasible experiment. A new attempt to detect neutron-rich Λ hypernuclei produced by stopped kaons is carried out now at DAΦNE [23]. The next stage is expected when J-PARC will start, where the serious program of study of neutron-rich Λ hypernuclei is scheduled [26]. Therefore, one may expect that the exploratory study will be followed by systematic extension of the hypernuclear chart towards the drip lines.

This work was strongly stimulated by numerous discussion with Y. Akaishi, L. Majling, T. Motoba, Khin Swe Myint, Y. Yamamoto, who also studied theoretically some aspects of neutron-rich hypernuclei. We are grateful to T. Fukuda, P.K. Saha and KEK E521 collaboration whose experimental activity greatly encouraged us in our study. We are indebted also to V. Paticchio and other members of FINUDA collaboration concerned with production of neutron-rich hypernuclei. This work is supported partially by Russian National Program for leading scientific schools, Grant 1619.2003.2.

References

[1] T.Yu. Tretyakova, D.E. Lanskoy, Eur.Phys.J. A5 (1999) 391
[2] Y. Yamamoto, H. Bandō, J. Žofka, Prog.Theor.Phys. 80 (1988) 757
[3] F. Fernández, T. López-Arias, C. Prieto, Z.Phys. A334 (1989) 349
[4] M. Rayet, Nucl.Phys. A367 (1981) 381
[5] E. Hiyama, M. Kamimura, T. Motoba, T. Yamada, Y. Yamamoto, Prog.Theor.Phys. 97 (1997) 881
[6] T. Motoba, Nucl.Phys. A547 (1992) 379c
[7] K. Tanida et al., Phys.Rev.Lett. 86 (2001) 1982
[8] L. Majling, Preprint JINR Dubna E2-92-442, 1992; Nucl.Phys. A585 (1995) 211c
[9] P.K. Saha et al., Phys.Rev.Lett. (in press)
[10] Y. Akaishi, T. Harada, S. Shinmura, Khin Swe Myint, Phys.Rev.Lett. 84 (2000) 3539
[11] S. Shinmura, Khin Swe Myint, T. Harada, Y. Akaishi, J.Phys. G28 (2002) 1
[12] D.E. Lanskoy, Y. Yamamoto, Phys.Rev. C55 (1997) 2330.
[13] M.M. Nagels, Th.A. Rijken, J.J. de Swart, Phys.Rev. D15 (1977) 2547
[14] M. Kohno, Prog.Theor.Phys. 88 (1992) 537
[15] P.M.M. Maessen, Th.A. Rijken, J.J. de Swart, Phys. Rev. C 40 (1989) 2226
[16] C.J. Batty, E. Friedman, A. Gal, Phys.Rep. 287 (1997) 385
[17] E. Hiyama, M. Kamimura, T. Motoba, T. Yamada, Y. Yamamoto, Phys.Rev. C65 (2002) 011301
[18] J. Hüfner, S.Y. Lee, H.A. Weidenmuller, Nucl.Phys. A234 (1974) 429
[19] A. Gal, L. Klieb, Phys.Rev. C34 (1986) 936
[20] T.Yu. Tretyakova, D.E. Lanskoy, Nucl.Phys. A691 (2001) 51c
[21] H. Tamura, R.S. Hayano, H. Outa, T. Yamazaki, Prog.Theor.Phys. Suppl. 117 (1994) 1
[22] K. Kubota et al., Nucl.Phys. A602 (1996) 327
[23] S. Marcello, III Int. Workshop on Nucl. and Part. Phys. at J-PARC (NP2004), 2-4 Aug. 2004, Tokai, Japan. *http://www-ps.kek.jp/jhf-np/NP04/presentations/Strangeness/NP04_Marcello.pdf*
[24] H. Bandō, T. Motoba, J. Žofka, Int.J.Mod.Phys. A5 (1990) 4021
[25] T.Yu. Tretyakova, D.E. Lanskoy, Phys.At.Nucl. 66 (2003) 1651
[26] H. Noumi, T. Fukuda, P.K. Saha, High-resolution reaction spectroscopy of $S = -1$ hypernuclei, Letter of Intent LOI08, KEK, 2002; P.K. Saha, T. Fukuda, H. Noumi, Neutron-rich Λ hypernuclei by the double-charge exchange reaction, Letter of Intent LOI09, KEK, 2002.